OH-Initiated Atmospheric Degradation of Hydroxyalkyl Hydroperoxides: Mechanism, Kinetics, and Structure-Activity Relationship

Long Chen,[1,2] Yu Huang, *,[1,2] Yonggang Xue, [1,2] Zhihui Jia,[3] Wenliang Wang[4]

[1] *State Key Lab of Loess and Quaternary Geology (SKLLQG), Institute of Earth Environment, Chinese Academy of Sciences (CAS), Xi'an, 710061, China*

[2] *CAS Center for Excellence in Quaternary Science and Global Change, Xi'an, 710061, China*

[3] *School of Materials Science and Engineering, Shaanxi Normal University, Xi'an, Shaanxi, 710119, China*

[4] *School of Chemistry and Chemical Engineering, Key Laboratory for Macromolecular Science of Shaanxi Province, Shaanxi Normal University, Xi'an, Shaanxi, 710119, China*

Submitted to *Atmospheric Chemistry & Physics*

*Corresponding author:

Prof. Yu Huang, E-mail address: huangyu@ieecas.cn

Contents:

Table S13 Rate coefficients of R32 and R33 in the $HOCH_3CHOO\cdot$ + NO system computed at different temperatures

Table S14 Rate coefficients of R38 and R39 in the $HO(CH_3)_2COO\cdot$ + NO system computed at different temperatures

Figure S1. PES ($\Delta G_a^{\#}$ and $\Delta E_a^{\#}$, in italics) for the autoxidation of $HOCH_3CHOO$ radical predicted at the M06-2X/ma-TZVP//M06-2X/6-311+G(2df,2p) level of theory

Figure S2. PES ($\Delta G_a^{\#}$ and $\Delta E_a^{\#}$, in italics) for the autoxidation of $HO(CH_3)_2COO$ radical predicted at the M06-2X/ma-TZVP//M06-2X/6-311+G(2df,2p) level of theory

Table S1 Y//X (Y = M06-2X, CCSD(T), X = 6-311+G(2df,2p), ma-TZVP) calculated energy barrier ($\Delta E_a^{\#}$, $\Delta G_a^{\#}$) for ·OH + HHPs reactions based on the M06-2X/6-311+G(2df,2p) optimized geometries (kcal·mol^{-1})

Entry	CCSD(T)/6-311+G(2df,2p)		ma-TZVP	
	$\Delta E_a^{\#}$	$\Delta G_a^{\#}$	$\Delta E_a^{\#}$	$\Delta G_a^{\#}$
HO-CH_2OOH + ·OH				
R1(O_1-H_1)	6.0	6.4	6.1	6.4
R2(C_1-H_1)	5.0	5.3	5.3	5.1
R3(C_1-H_2)	4.4	5.6	4.6	5.8
R4(O_3-H_2)	1.1	2.1	0.5	1.5
HO-$CH(CH_3)OOH$ + ·OH				
R1'(O_1-H_1)	6.5	7.1	6.5	7.2
R2'(C_1-H)	0.5	1.4	1.3	2.2
R3'(-CH_3(R1))	4.9	6.2	4.6	5.9
R4'(O_3-H_2)	0.7	2.0	0.3	1.7
HO-$C(CH_3)_2OOH$ + ·OH				
R1"(O_1-H_1)	6.4	7.0	6.7	7.4
R2"(-CH_3(R1))	6.9	7.4	7.5	8.0
R3"(-CH_3(R2))	5.2	5.9	5.1	5.8
R4"(O_3-H_2)	4.7	5.1	5.2	5.5

Table S2 Rate coefficients (cm^3 $molecule^{-1}$ s^{-1}) of every elementary pathway and their branching ratios (Γ) involved in the initial reaction of HO-CH_2OO-H with OH radical computed at different temperatures

T/K	R1(O_1-H_1)	R2(C_1-H_1)	R3(C_1-H_2)	R4(O_3-H_2)	k_{tot}
273	2.9×10^{-12}	1.6×10^{-13}	3.0×10^{-13}	4.5×10^{-11}	4.8×10^{-11}
280	2.3×10^{-12}	1.5×10^{-13}	2.7×10^{-13}	3.6×10^{-11}	3.9×10^{-11}
298	1.8×10^{-12}	1.4×10^{-13}	2.6×10^{-13}	2.9×10^{-11}	3.2×10^{-11}
300	1.5×10^{-12}	1.3×10^{-13}	2.4×10^{-13}	2.4×10^{-11}	2.6×10^{-11}
320	1.1×10^{-12}	1.1×10^{-13}	2.3×10^{-13}	1.7×10^{-11}	1.9×10^{-11}
340	8.6×10^{-13}	9.5×10^{-14}	2.2×10^{-13}	1.3×10^{-11}	1.4×10^{-11}
360	7.2×10^{-13}	8.2×10^{-14}	2.1×10^{-13}	1.0×10^{-11}	1.1×10^{-11}
380	6.2×10^{-13}	7.1×10^{-14}	2.1×10^{-13}	8.2×10^{-12}	9.1×10^{-12}
400	5.6×10^{-13}	6.2×10^{-14}	2.1×10^{-13}	6.8×10^{-12}	7.6×10^{-12}

T/K	$\Gamma_{R1(O1-H1)}$(%)	$\Gamma_{R2(C1-H1)}$(%)	$\Gamma_{R3(C1-H2)}$(%)	$\Gamma_{R4(O3-H2)}$(%)
273	5.97	0.32	0.61	93.09
280	5.83	0.38	0.71	93.08
298	5.76	0.43	0.81	92.99
300	5.74	0.49	0.93	92.84
320	5.84	0.58	1.21	92.37
340	6.07	0.67	1.53	91.73
360	6.41	0.73	1.91	90.95
380	6.84	0.78	2.34	90.04
400	7.34	0.81	2.82	89.03

Table S3 Rate coefficients (cm^3 $molecule^{-1}$ s^{-1}) of every elementary pathway and their branching ratios (Γ) involved in the initial reaction of HO-CH(CH_3)OOH with OH radical computed at different temperatures

T/K	R1'(O_1-H_1)	R2'(C_1-H)	R3'(-CH_3(R1))	R4'(O_3-H_2)	k'_{tot}
273	3.8×10^{-12}	1.1×10^{-12}	4.6×10^{-14}	4.2×10^{-11}	4.7×10^{-11}
280	2.9×10^{-12}	1.0×10^{-12}	4.4×10^{-14}	3.4×10^{-11}	3.8×10^{-11}
298	2.3×10^{-12}	9.5×10^{-13}	4.2×10^{-14}	2.8×10^{-11}	3.1×10^{-11}
300	1.9×10^{-12}	9.0×10^{-13}	4.0×10^{-14}	2.3×10^{-11}	2.6×10^{-11}
320	1.3×10^{-12}	8.3×10^{-13}	3.7×10^{-14}	1.7×10^{-11}	1.9×10^{-11}
340	1.0×10^{-12}	7.7×10^{-13}	3.4×10^{-14}	1.3×10^{-11}	1.4×10^{-11}
360	8.2×10^{-13}	7.4×10^{-13}	3.1×10^{-14}	9.8×10^{-12}	1.1×10^{-11}
380	7.0×10^{-13}	7.1×10^{-13}	2.9×10^{-14}	7.9×10^{-12}	9.4×10^{-12}
400	6.2×10^{-13}	6.9×10^{-13}	2.8×10^{-14}	6.6×10^{-12}	7.9×10^{-12}

T/K	$\Gamma_{R1'(O1-H1)}$(%)	$\Gamma_{R2'(C1-H)}$(%)	$\Gamma_{R3'(-CH3(R1))}$(%)	$\Gamma_{R4'(O3-H2)}$(%)
273	8.10	2.32	0.10	89.51
280	7.69	2.68	0.12	89.48
298	7.39	3.08	0.14	89.40
300	7.19	3.49	0.16	89.16
320	7.00	4.40	0.20	88.40
340	7.02	5.40	0.24	87.35
360	7.19	6.46	0.27	86.08
380	7.46	7.56	0.31	84.66
400	7.81	8.69	0.35	83.15

Table S4 Rate coefficients (cm^3 $molecule^{-1}$ s^{-1}) of every elementary pathway and their branching ratios (Γ) involved in the initial reaction of HO-C(CH_3)$_2$OOH with OH radical computed at different temperatures

T/K	R1"(O_1-H_1)	R2"(-CH_3(R1))	R3"(-CH_3(R2))	R4"(O_3-H_2)	k"$_{tot}$
273	2.5×10^{-12}	3.8×10^{-14}	2.5×10^{-14}	8.0×10^{-12}	1.1×10^{-11}
280	1.9×10^{-12}	3.7×10^{-14}	2.5×10^{-14}	6.5×10^{-12}	8.4×10^{-12}
298	1.5×10^{-12}	3.6×10^{-14}	2.3×10^{-14}	5.4×10^{-12}	6.9×10^{-12}
300	1.2×10^{-12}	3.5×10^{-14}	2.3×10^{-14}	4.6×10^{-12}	5.8×10^{-12}
320	8.5×10^{-13}	3.3×10^{-14}	2.2×10^{-14}	3.5×10^{-12}	4.4×10^{-12}
340	6.4×10^{-13}	3.1×10^{-14}	2.2×10^{-14}	2.8×10^{-12}	3.5×10^{-12}
360	5.2×10^{-13}	2.9×10^{-14}	2.1×10^{-14}	2.4×10^{-12}	2.9×10^{-12}
380	4.4×10^{-13}	2.8×10^{-14}	2.1×10^{-14}	2.1×10^{-12}	2.5×10^{-12}
400	3.8×10^{-13}	2.7×10^{-14}	2.0×10^{-14}	1.8×10^{-12}	2.2×10^{-12}

T/K	$\Gamma_{R1"(O1-H1)}$(%)	$\Gamma_{R2"(-CH3(R1))}$(%)	$\Gamma_{R3"(-CH3(R2))}$(%)	$\Gamma_{R4"(O3-H2)}$(%)
273	23.74	0.36	0.24	75.66
280	22.55	0.44	0.28	76.73
298	21.52	0.52	0.33	77.62
300	20.64	0.60	0.39	78.37
320	19.26	0.75	0.51	79.49
340	18.28	0.88	0.63	80.22
360	17.61	0.99	0.73	80.66
380	17.18	1.10	0.84	80.88
400	16.93	1.21	0.93	80.93

Table S5 Rate coefficients (cm^3 $molecule^{-1}$ s^{-1}) of HO_2 radical reactions with $HOCH_2OO$ (R19), $HOCH_3CHOO$ (R20) and $HO(CH_3)_2COO$ radicals (R21) computed at different temperatures

T/K	R19	R20	R21
273	3.1×10^{-11}	9.1×10^{-11}	1.5×10^{-10}
280	2.3×10^{-11}	6.4×10^{-11}	1.0×10^{-10}
298	1.7×10^{-11}	4.6×10^{-11}	7.4×10^{-11}
300	1.3×10^{-11}	3.4×10^{-11}	5.3×10^{-11}
320	8.1×10^{-12}	2.0×10^{-11}	3.0×10^{-11}
340	5.4×10^{-12}	1.2×10^{-11}	1.8×10^{-11}
360	3.8×10^{-12}	8.3×10^{-12}	1.2×10^{-11}
380	2.8×10^{-12}	5.8×10^{-12}	8.3×10^{-12}
400	2.1×10^{-12}	4.2×10^{-12}	5.9×10^{-12}

Table S6 The relative free energy and Boltzmann populations (w_i) of the conformer of $HOCH_2OO$ radical at the M06-2X/6-311+G(2df,2p) level of theory

Conformer	ΔG(kcal mol^{-1})	w_i
$HOCH_2OO$-a	0.000	46.39%
$HOCH_2OO$-b	0.001	46.31%
$HOCH_2OO$-c	1.623	2.99%
$HOCH_2OO$-d	1.406	4.32%

Table S7 The single-conformer rate coefficients ($k_{IRC\text{-}TST}$) and multi-conformer rate coefficients ($k_{MC\text{-}TST}$) of $HOCH_2OO$ radical computed at different temperatures

T/K	$k_{IRC\text{-}TST}$(TS22-a)	$k_{IRC\text{-}TST}$(TS22-b1)	$k_{IRC\text{-}TST}$(TS22-b2)	$k_{MC\text{-}TST}$
273	1.9×10^{-17}	2.1×10^{-17}	6.6×10^{-20}	1.8×10^{-17}
280	9.5×10^{-17}	1.0×10^{-16}	3.8×10^{-19}	9.1×10^{-17}
298	4.6×10^{-16}	4.8×10^{-16}	2.1×10^{-18}	4.4×10^{-16}
300	2.2×10^{-15}	2.3×10^{-15}	1.1×10^{-17}	2.0×10^{-15}
320	4.3×10^{-14}	4.4×10^{-14}	2.7×10^{-16}	4.1×10^{-14}
340	7.6×10^{-13}	7.7×10^{-13}	6.0×10^{-15}	7.1×10^{-13}
360	1.2×10^{-11}	1.2×10^{-11}	1.1×10^{-13}	1.1×10^{-11}
380	1.5×10^{-10}	1.5×10^{-10}	1.8×10^{-12}	1.4×10^{-10}
400	1.6×10^{-09}	1.6×10^{-09}	2.4×10^{-11}	1.5×10^{-09}

Table S8 The relative free energy and Boltzmann populations (w_i) of the conformer of $HOCH_3CHOO$ radical at the M06-2X/6-311+G(2df,2p) level of theory

Conformer	ΔG(kcal·mol^{-1})	w_i
$HOCH_3CHOO$-a	0.000	80.13%
$HOCH_3CHOO$-b	0.942	16.33%
$HOCH_3CHOO$-c	2.218	1.89%
$HOCH_3CHOO$-d	2.299	1.65%

Table S9 The single-conformer rate coefficients ($k_{IRC\text{-}TST}$) and multi-conformer rate coefficients ($k_{MC\text{-}TST}$) of $HOCH_3CHOO$ radical computed at different temperatures

T/K	$k_{IRC\text{-}TST}$(TS23-a)	$k_{IRC\text{-}TST}$(TS23-b)	$k_{IRC\text{-}TST}$(TS23-c1)	$k_{IRC\text{-}TST}$(TS23-c2)	$k'_{MC\text{-}TST}$
273	8.0×10^{-18}	8.3×10^{-14}	3.3×10^{-18}	1.8×10^{-13}	1.7×10^{-14}
280	4.3×10^{-17}	3.5×10^{-13}	1.5×10^{-17}	7.9×10^{-13}	7.2×10^{-14}
298	2.3×10^{-16}	1.4×10^{-12}	6.9×10^{-17}	3.3×10^{-12}	2.9×10^{-13}
300	1.2×10^{-15}	5.1×10^{-12}	3.1×10^{-16}	1.3×10^{-11}	1.1×10^{-12}
320	2.6×10^{-14}	5.8×10^{-11}	6.1×10^{-15}	1.5×10^{-10}	1.2×10^{-11}
340	5.2×10^{-13}	5.5×10^{-10}	1.1×10^{-13}	1.6×10^{-9}	1.2×10^{-10}
360	8.6×10^{-12}	4.5×10^{-09}	1.8×10^{-12}	1.3×10^{-8}	9.8×10^{-10}
380	1.2×10^{-10}	3.2×10^{-08}	2.5×10^{-11}	9.7×10^{-8}	7.1×10^{-9}
400	1.3×10^{-9}	2.0×10^{-7}	3.0×10^{-10}	6.3×10^{-7}	4.6×10^{-8}

Table S10 The relative free energy and Boltzmann populations (w_i) of the conformer of $HO(CH_3)_2COO$ radical at the M06-2X/6-311+G(2df,2p) level of theory

Conformer	ΔG(kcal·mol^{-1})	w_i
$HO(CH_3)_2COO$-a	0.000	88.04%
$HO(CH_3)_2COO$-b	1.334	9.25%
$HO(CH_3)_2COO$-c	2.062	2.71%

Table S11 The single-conformer rate coefficients ($k_{IRC\text{-}TST}$) and multi-conformer rate coefficients ($k_{MC\text{-}TST}$) of $HO(CH_3)_2COO$ radical computed at different temperatures

T/K	$k_{IRC\text{-}TST}$(TS24-a)	$k_{IRC\text{-}TST}$(TS24-b1)	$k_{IRC\text{-}TST}$(TS24-b2)	$k_{IRC\text{-}TST}$(TS24-c)	$k''_{MC\text{-}TST}$
273	1.4×10^{-13}	1.2×10^{-13}	2.0×10^{-14}	1.6×10^{-12}	1.8×10^{-13}
280	6.1×10^{-13}	5.7×10^{-13}	9.0×10^{-14}	6.2×10^{-12}	7.7×10^{-13}
298	2.5×10^{-12}	2.4×10^{-12}	3.9×10^{-13}	2.3×10^{-11}	3.0×10^{-12}
300	9.2×10^{-12}	9.6×10^{-12}	1.5×10^{-12}	8.0×10^{-11}	1.1×10^{-11}
320	1.1×10^{-10}	1.2×10^{-10}	2.0×10^{-11}	8.3×10^{-10}	1.3×10^{-10}
340	1.1×10^{-9}	1.3×10^{-9}	2.2×10^{-10}	7.2×10^{-9}	1.3×10^{-9}
360	8.7×10^{-9}	1.1×10^{-8}	1.9×10^{-9}	5.3×10^{-8}	1.0×10^{-8}
380	6.3×10^{-8}	8.3×10^{-8}	1.5×10^{-8}	3.5×10^{-7}	7.4×10^{-8}
400	4.1×10^{-7}	5.4×10^{-7}	1.0×10^{-7}	2.1×10^{-6}	4.7×10^{-7}

Table S12 Rate coefficients of R27 and R29 in the $HOCH_2OO\cdot$ + NO system computed at different temperatures

T/K	k_{R27}	k_{R29}
273	5.1×10^{-12}	4.3×10^{-18}
280	4.9×10^{-12}	5.0×10^{-18}
298	4.3×10^{-12}	7.6×10^{-18}
300	4.2×10^{-12}	7.9×10^{-18}
320	3.5×10^{-12}	1.2×10^{-17}
340	2.2×10^{-12}	1.8×10^{-17}
360	1.8×10^{-12}	2.6×10^{-17}
380	1.4×10^{-12}	3.7×10^{-17}
400	1.3×10^{-12}	5.1×10^{-17}

Table S13 Rate coefficients of R32 and R33 in the $HOCH_3CHOO\cdot$ + NO system computed at different temperatures

T/K	k_{R32}	k_{R33}
273	7.6×10^{-12}	2.0×10^{6}
280	5.8×10^{-12}	2.9×10^{6}
298	4.3×10^{-12}	7.3×10^{6}
300	4.2×10^{-12}	8.1×10^{6}
320	3.8×10^{-12}	1.9×10^{7}
340	2.7×10^{-12}	4.4×10^{7}
360	1.9×10^{-12}	9.0×10^{7}
380	1.4×10^{-12}	1.7×10^{8}
400	1.1×10^{-12}	3.1×10^{8}

Table S14 Rate coefficients of R38 and R39 in the $HO(CH_3)_2COO\cdot$ + NO system computed at different temperatures

T/K	k_{R38}	k_{R39}
273	7.9×10^{-12}	2.6×10^{6}
280	6.3×10^{-12}	3.8×10^{6}
298	4.8×10^{-12}	9.5×10^{6}
300	4.7×10^{-12}	1.0×10^{7}
320	3.2×10^{-12}	2.5×10^{7}
340	2.6×10^{-12}	5.6×10^{7}
360	1.9×10^{-12}	1.1×10^{8}
380	1.7×10^{-12}	2.2×10^{8}
400	1.5×10^{-12}	3.8×10^{8}

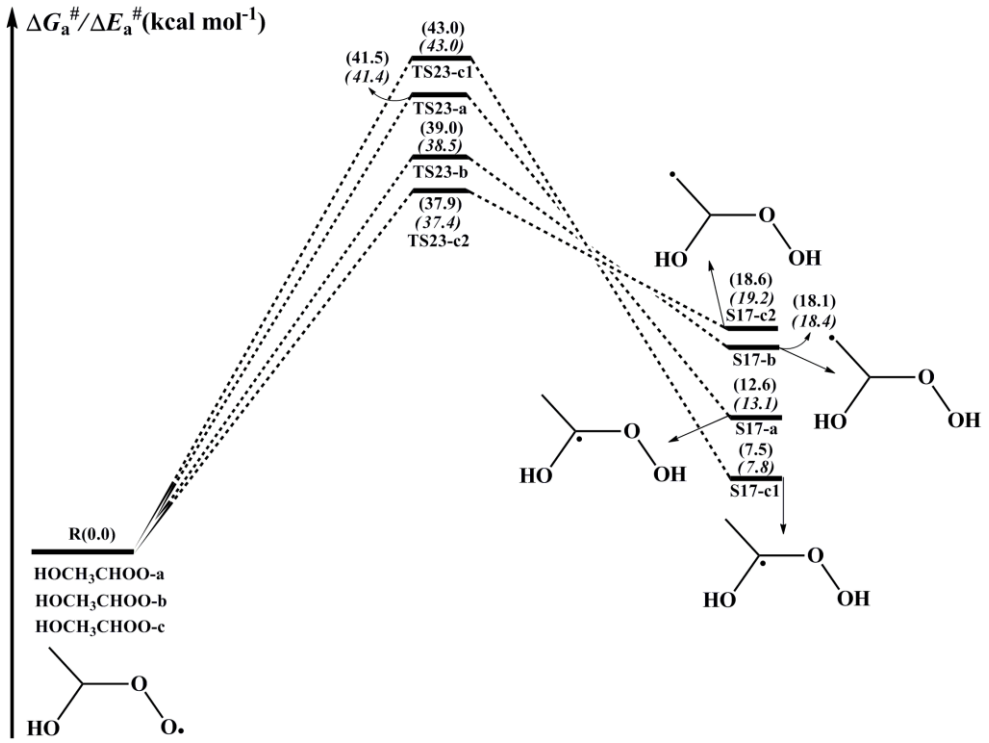

Figure S1. PES ($\Delta G_a^{\#}$ and $\Delta E_a^{\#}$, in italics) for the autoxidation of $HOCH_3CHOO$ radical predicted at the M06-2X/ma-TZVP//M06-2X/6-311+G(2df,2p) level of theory

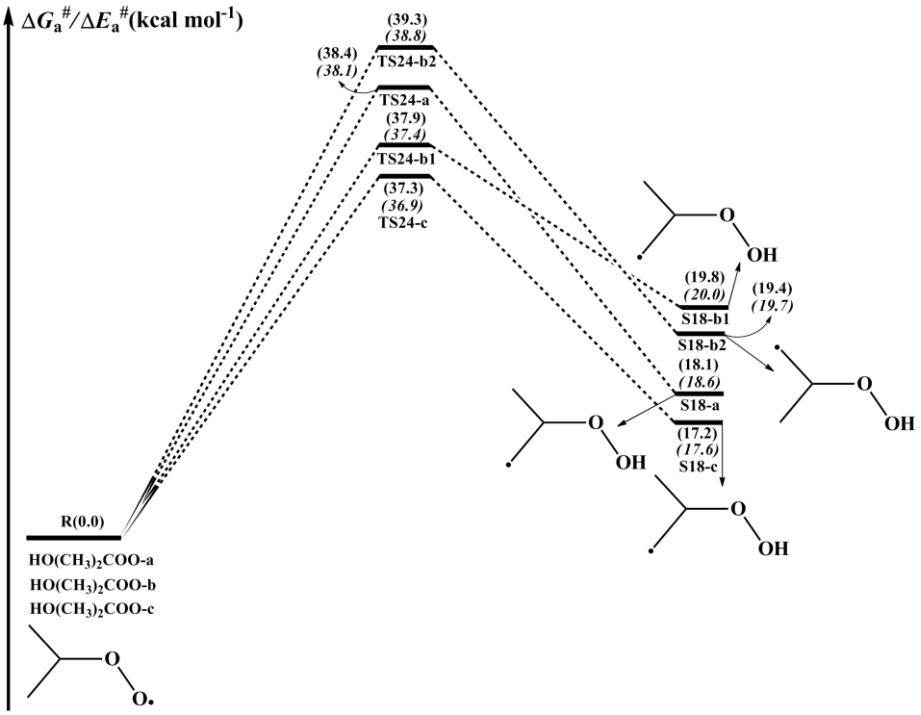

Figure S2. PES ($\Delta G_a^{\#}$ and $\Delta E_a^{\#}$, in italics) for the autoxidation of $HO(CH_3)_2COO$ radical predicted at the M06-2X/ma-TZVP//M06-2X/6-311+G(2df,2p) level of theory